

refractive index can be written in terms of the stress-optical coefficients as

$$\Delta n = \frac{1}{2}n^3(AP + BP^2), \quad (4)$$

where P represents the stress, and A and B are combinations of the first- and second-order piezo-optical coefficients. They have the following values for the ordinary ray:

$$A_\omega = q_{11} + q_{12} + q_{13}, \quad (5)$$

$B_\omega = 2q_{111} + 2q_{112} + q_{211} - q_{222} + 2q_{113} + 2q_{123} + q_{133}$, (6)
and for the extraordinary ray:

$$A_e = 2q_{31} + q_{33}, \quad (7)$$

$$B_e = 2q_{311} + 2q_{312} + 4q_{313} + q_{333}, \quad (8)$$

where q_{ij} and q_{ijk} are the first- and second-order piezo-optical coefficients. A similar set of equations can be written relating Δn and the strains in terms of the first- and second-order elasto-optic coefficients.

By least-squares fit of the experimental data the values of A and B were evaluated for all these crystals and are entered in Table IV.

The individual values of the second-order stress-optical tensor components cannot be evaluated from the above analysis, but the importance of the second-order coefficients is demonstrated. This is the first time such nonlinear behavior has been observed in noncubic crystals. Since the observed fringe shifts upon increasing and upon releasing the pressure matched to within a fraction of a fringe, it may be concluded that the above nonlinear behavior occurred in the elastic region.

Amplitude-Dependent Ultrasonic Attenuation in n -InSb at Liquid-Helium Temperatures

T. ISHIGURO AND N. MIKOSHIBA

Electrotechnical Laboratory, Tanashi, Tokyo, Japan

(Received 5 December 1968)

Ultrasonic attenuation which strongly depends on the amplitude of ultrasonic waves was observed in Ge-doped n -InSb at liquid-helium temperatures and in magnetic fields perpendicular to the propagation direction. The measurements were performed with 43- and 160-MHz shear waves propagating along the $[110]$ direction and polarized in the $[001]$ direction. This anomalous attenuation is explained mainly by the ultrasonic-wave-induced non-Ohmic behavior due to the repopulation of carriers between conduction and impurity bands.

INTRODUCTION

ULTRASONIC attenuations in solids reported so far are usually independent of the amplitude of ultrasonic waves and discussed by using the theory of linear response or the small-signal theory. However, an amplitude-dependent attenuation due to dislocations has been recently observed in superconductors.¹ We report a strongly amplitude-dependent ultrasonic attenuation in n -InSb at liquid-helium temperatures.

The ultrasonic attenuation due to conduction electrons in piezoelectric semiconductors has been observed for piezoelectrically active modes.² Since this attenuation depends on the carrier concentration and the mobility, one can control the attenuation by applying

lights² (photoconducting CdS) or magnetic fields³ (InSb, GaAs) and can distinguish the electronic loss from the other loss due to dislocations, thermal phonons, mode conversions at boundaries, etc. In the case of change in carrier mobility by an external magnetic field, the difference in the attenuation coefficient with and without a magnetic field $[\alpha(H) - \alpha(0)]$ can be directly compared with the theory of electronic attenuation. If the resistivity of samples is measured, such a comparison gives a good estimation of the drift mobility of carriers. As the carrier mobility is very large ($\mu \gtrsim 10^5$ cm²/V sec) in n -InSb, a strong dependence of ultrasonic attenuation on the magnetic fields can be observed even in magnetic fields less than 10 kG.³

The piezoelectric field accompanying ultrasonic waves is estimated by the Hutson-White theory.⁴ For example, in n -InSb of resistivity $\rho = 50$ Ω cm and carrier mobility $\mu = 10^5$ cm²/V sec, the amplitude of the piezoelectric field becomes about 0.5 V/cm for an ultrasonic wave of

¹ R. E. Love and R. W. Shaw, *Rev. Mod. Phys.* **34**, 260 (1964); R. E. Love, R. W. Shaw, and W. A. Fate, *Phys. Rev.* **138**, A1453 (1965); B. R. Tittman and H. E. Bömmel, *ibid.* **151**, 178 (1966); A. Hikata, R. A. Johnson, and C. Elbaum, *Phys. Rev. Letters* **17**, 916 (1966); A. Hikata and C. Elbaum, *ibid.* **18**, 750 (1967); W. P. Mason, *Phys. Rev.* **143**, 229 (1966).

² H. D. Nine and R. Truell, *Phys. Rev.* **132**, 799 (1961); A. R. Hutson, J. H. McFee, and D. L. White, *Phys. Rev. Letters* **7**, 237 (1961); T. Ogawa, *J. Phys. Soc. Japan* **17**, 400 (1962).

³ T. Ishiguro, Y. Abe, and N. Mikoshiba, in *Reports of the Sixth International Congress on Acoustics* (Acoustical Society of Japan, Tokyo, 1968), p. H-109.

⁴ A. R. Hutson and D. L. White, *J. Appl. Phys.* **33**, 40 (1962).

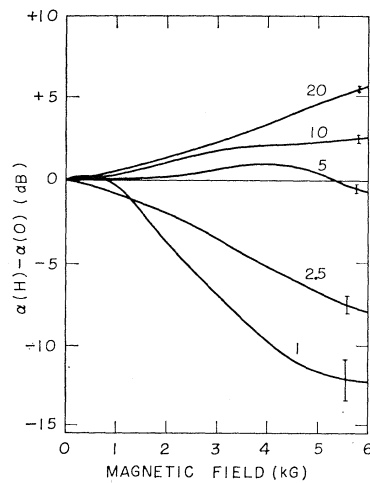


FIG. 1. Magnetic-field dependence of attenuation for the ultrasonic wave of 160 MHz at 1.5°K for various amplitudes. The number given for each curve indicates the amplitude in an arbitrary unit. The path length of the wave was 29.8 mm. The fluctuation level of the signal is shown by the length of the straight line.

160 MHz and power density 10 mW/cm². This value is sufficiently large to induce non-Ohmic behavior in *n*-InSb at liquid-helium temperatures.^{5,6} When the wavelength of ultrasonic wave is much larger than the mean free path of electrons and the period of ultrasonic waves is much longer than the build-up time of non-Ohmic conduction, the ultrasonic waves feel the dc limit of resistivity.⁷

We present experimental results and discussion on the amplitude-dependent ultrasonic attenuation in *n*-InSb due to the ultrasonic-wave-induced non-Ohmic conduction.

EXPERIMENTAL

A sample was cut out of an ingot of Ge-doped InSb. The sample has the mobility of 2.74×10^5 cm²/V sec and

⁵ See, for the experiments which show the non-Ohmic conduction in *n*-InSb due to the hot electron effect, E. H. Putley, in *Proceedings of the Seventh International Conference on the Physics of Semiconductors, Paris, 1964* (Academic Press Inc., New York, 1964), p. 443; K. Komatsubara and E. Yamada, *Phys. Rev.* **144**, 702 (1966); N. Kotera, K. Komatsubara, and E. Yamada, *J. Phys. Soc. Japan Suppl.* **21**, 411 (1966).

⁶ See, for the experiments which show the non-Ohmic conduction in *n*-InSb due to the repopulation of electrons between the impurity and the conduction bands, Lien Chih-ch'ao and D. N. Nasledov, *Fiz. Tverd. Tela* **2**, 793 (1960) [English transl.: *Soviet Phys.—Solid State* **2**, 729 (1960)]; V. A. Danilychev, *Zh. Eksperim. i Teor. Fiz. Pis'ma v Redaktsiyu* **2**, 482 (1965) [English transl.: *Soviet Phys.—JETP Letters* **2**, 300 (1965)]; H. Miyazawa and H. Ikoma, *J. Phys. Soc. Japan* **23**, 290 (1967).

⁷ Production of hot electrons by strong hypersonic waves ($ql \gg 1$, where q is the wave number of the wave, and l is the mean free path of electrons) has been discussed in the following articles: B. V. Paranjape, *Physica* **30**, 1641 (1964); E. M. Epshtein, *Fiz. Tverd. Tela* **8**, 552 (1966) [English transl.: *Soviet Phys.—Solid State* **8**, 436 (1966)]; S. Tanaka, S. Asai, and M. Kogami, in *Proceedings of the Ninth International Conference on Physics of Semiconductors, Moscow, 1968*, edited by S. M. Ryvkin (Nauka Publishing House, Leningrad, 1968), p. 779. As our measurement was performed in the low-frequency range ($ql \ll 1$), we analyzed the data in a different way.

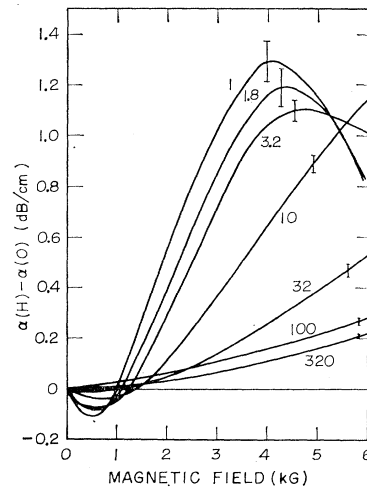


FIG. 2. Magnetic-field dependence of attenuation for the ultrasonic wave of 43 MHz at 4.2°K for various amplitudes. The number given for each curve indicates the amplitude in an arbitrary unit. The fluctuation level of the signal is shown by the length of the straight line.

the carrier concentration of 1.5×10^{13} cm⁻³ at 77°K. The dimensions of the sample were $14.9 \times 1.7 \times 2.2$ mm³; the longest side was parallel to the [110] direction. The ultrasonic wave was polarized in the [001] direction and propagated along the [110] direction so as to produce the piezoelectric field, and the magnetic field was applied in the (110) plane. The ultrasonic attenuation was measured by using standard pulse-echo techniques in the frequency range 15–305 MHz and the temperature range 1.5–4.2°K. A boxcar integrator allowed the continuous recording of a particular echo amplitude as a function of magnetic field. The value of $\alpha(H) - \alpha(0)$ was then obtained by taking the relative value of the echo to that in the absence of the magnetic field. An exciting rf pulse was passed through a calibrated attenuator into a transducer.

Since the acoustic characteristic of a bond between a quartz transducer and the sample seems rather insensitive to temperature between 1.5 and 77°K, the absolute values of the acoustic power were estimated by measuring the acoustoelectric effect at 77°K where the attenuation was independent of the amplitude. The pulsed acoustoelectric voltages were picked up with and without the magnetic field by a pair of contacts whose separation was less than the length of wave train.⁸ According to the Weinreich relation,⁸ the acoustic power P is given in terms of the difference in the acoustoelectric field with and without the magnetic field $E_{ae}(H) - E_{ae}(0)$ and the difference in the attenuation coefficient $\alpha(H) - \alpha(0)$:

$$P = qnv_s A [E_{ae}(H) - E_{ae}(0)] / [\alpha(H) - \alpha(0)],$$

where q is the charge of an electron, n is the carrier con-

⁸ J. R. A. Beale and M. Pomerantz, *Phys. Rev. Letters* **13**, 198 (1964). See also G. Weinreich, T. M. Sanders, and H. G. White, *Phys. Rev.* **114**, 33 (1959).

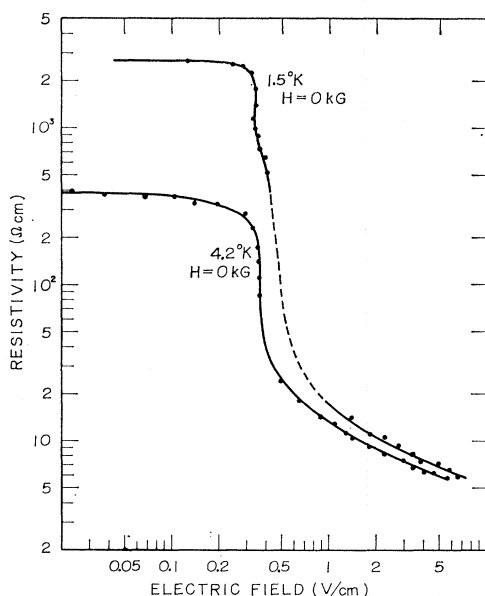


FIG. 3. Electric field dependence of dc resistivity of the sample at 4.2 and 1.5°K.

centration, A is the cross section of the sample, and v_s is the velocity of sound.

A typical example of the magnetic field dependence of the attenuation coefficient $\alpha(H) - \alpha(0)$ is shown for various amplitudes in Fig. 1 for the frequency of 160 MHz at 1.5°K. The fluctuation level of the signal is shown by the length of the straight line for each curve in Fig. 1. Though the amplitude is expressed in an arbitrary unit and increases with numbers in Fig. 1, the input power estimated by the acoustoelectric effect was 0.12 ± 0.02 mW for unit amplitude. In the small amplitude case, $\alpha(H) - \alpha(0)$ decreases with increasing magnetic field, while it increases in the large amplitude case. This amplitude dependence of attenuation is not ascribed to heating of the lattice by the ultrasonic wave, since the characteristics of the attenuation were independent of both the pulse width and the repetition rate in our measuring condition. It is noted here, also, that the amplitude-dependent attenuation was not observed for ultrasonic waves which do not produce the piezoelectric field.

Although the amplitude dependence of $\alpha(H) - \alpha(0)$ is quite strong in Fig. 1, it is difficult to discuss quantitatively the amplitude dependence for the wave of 160 MHz because the attenuation is so large that the wave feels different conditions for attenuation, i.e., different resistivities throughout the sample. Hence, we shall take the experimental data for 43 MHz at 4.2°K for quantitative discussions. The reasons for this choice are as follows: First, the attenuation is sufficiently small ($\alpha \lesssim 1$ dB/cm) that the physical situation is uniform over the sample. Second, the freeze-out effect⁹ can be

⁹ See, for instance, E. H. Putley, in *Semiconductors and Semimetals*, edited R. K. Willardson and A. C. Beer (Academic Press Inc., New York, 1966), Vol. 1, p. 289.

TABLE I. Acoustic power P and the corresponding piezoelectric field without the screening factor F_s [see Eq. (3)].

Frequency (MHz)	Acoustic power P (mW)	$e\Delta/\epsilon$ (V/cm)
160	50 (max)	70.6
	0.12 (min)	3.5
43	10^8 (max)	320
	10^{-2} (min)	1

neglected in magnetic fields less than 6 kG at 4.2°K, because the change in the Hall coefficient with magnetic field under the small electric field is less than 30% in magnetic fields between 1 and 6 kG. Third, the measurement of attenuation in a very wide amplitude range (~ 50 dB) is technically possible for 43 MHz. Figure 2 shows the experimental data of the magnetic field dependence of $\alpha(H) - \alpha(0)$ for 43 MHz at 4.2°K for various amplitudes. The numbers of curves indicate the relative values of amplitude and the power estimated by the acoustoelectric effect was $(1 \pm 0.1) \times 10^{-2}$ mW for unit amplitude. The fluctuation level is shown as in Fig. 1.

In Fig. 3 is shown the dc electric field dependence of resistivity of our sample at 1.5 and 4.2°K. The resistivity decreases by 2 to 3 orders of magnitude at $E \cong 0.4$ V/cm.

DISCUSSION

First, let us estimate the strain Δ and the amplitude of the ac electric field E_s accompanying the acoustic power P by using the following relations⁴:

$$P = \frac{1}{2} c_{44} \Delta^2 A v_s, \quad (1)$$

$$E_s = (e\Delta/\epsilon) F_s, \quad (2)$$

$$F_s = \frac{\{[1 + (\omega/\omega_D)(\omega_s/\omega + \omega/\omega_D)]^2 + (\omega_s/\omega)^2\}^{\frac{1}{2}}}{1 + (\omega_s/\omega + \omega/\omega_D)^2}, \quad (3)$$

where c_{44} is the elastic constant, ω is the angular frequency of the ultrasonic waves, ω_s is the dielectric relaxation frequency ($\omega_s = 1/\epsilon\rho$), ϵ is the dielectric constant, ω_D is the diffusion frequency ($\omega_D = qv_s^2/kT\mu$), and e is the piezoelectric constant.

The values of P , $e\Delta/\epsilon$, and F_s for our experimental arrangement are tabulated in Tables I and II by using the following numerical values: $c_{44} = 3.02 \times 10^{11}$

TABLE II. Screening factor F_s for the resistivities in the Ohmic and non-Ohmic regions. We assume $\mu = 10^6$ cm²/V sec.

Temperature (°K)	Resistivity (Ω cm)	F_s
1.5 ^a	2.7×10^3 (Ohmic)	0.89
	12 (non-Ohmic)	2.3×10^{-2}
4.2 ^b	3.8×10^2 (Ohmic)	0.15
	9 (non-Ohmic)	4×10^{-3}

^a For 160 MHz.

^b For 43 MHz.

dyn/cm², $A=3.7\times 10^{-2}$ cm², $v_s=2.29\times 10^5$ cm/sec, $e=0.06$ C/m², and $\epsilon=18.7$. Let us consider the amplitude dependence of attenuation for 43 MHz in Fig. 2. One can see from Tables I and II that when the maximum acoustic power, 10³ mW, is put into the sample at 4.2°K, $|E_s|$ becomes 48 V/cm if we use the resistivity in the Ohmic region. The value of 48 V/cm is of course sufficiently large to produce the non-Ohmic conduction. Therefore, we must use self-consistently the value of resistivity in the non-Ohmic region. For example, if the value of $\rho=9$ Ω cm is used, $|E_s|$ becomes about 1.3 V/cm. This $\rho-|E_s|$ relation is consistent with the non-Ohmic behavior in Fig. 3. In other words, the maximum acoustic power really brings the sample into the non-Ohmic region and gives rise to the amplitude dependence of attenuation.

Besides the ac piezoelectric field E_s , a dc acoustoelectric field appears in the sample during the propagation of ultrasonic waves. This dc field, however, does not contribute to the ac acceleration of carriers so long as the sample is in an open circuit, since the acoustoelectric field is the counter field to balance the "snow-drift" of carriers by ultrasonic waves.⁸

Let us now discuss the magnetic field dependence of attenuation. The attenuation coefficient in a transverse magnetic field is given by a straightforward extension¹⁰ of the Hutson-White theory⁴,

$$\alpha(H) = \frac{K^2\omega}{2v_s} \frac{(\omega/\omega_s)}{[(\omega/\omega_s)^2 + (1 + \omega^2/\omega_s\omega_D)^2]}, \quad (4)$$

where K is the electromechanical coupling constant and is 2.7×10^{-2} in our case. In magnetic fields higher than 1 kG, the conductivity and the mobility of the sample decrease with magnetic field due to the magnetoresistance. In this case the magnetic field dependence of $\alpha(H)$ is classified into two cases depending on the degree of screening effect.³ In the nearly complete screening case ($\omega \ll \omega_s$, $\omega^2/\omega_s\omega_D \lesssim 1$), the $\alpha(H)$ increases with increasing H , while in the incomplete screening case ($\omega \gg \omega_s$, $\omega^2/\omega_s\omega_D \lesssim 1$), the $\alpha(H)$ decreases with H . As Eq. (4) has been derived for the case where the resistivity is constant at any phase of oscillation of ultrasonic waves, we can apply Eq. (4) with confidence to the small amplitude limit of ultrasonic waves. Moreover, Eq. (4) holds approximately in the large-amplitude limit because the ultrasonic waves do not feel such sharply varying resistivity during the oscillation except for the short time of small strains. Therefore, we shall confine ourselves to the discussion of the small- and large-amplitude limits.

Before discussing quantitatively the experimental result in Fig. 2, the following two points should be noted: (1) The incomplete screening case does not occur for 43 MHz at 4.2°K because $\omega=2.7\times 10^8$ is much

smaller than $\omega_s (> 1.6\times 10^9)$; (2) the $\alpha(H)$ decreases at first with increasing magnetic field because of the negative magnetoresistance.¹¹ We will now take a two-band model⁶ (impurity and conduction bands) where the mobility of electrons in the conduction band is several times higher than that in the impurity band and the repopulation of electrons in these two bands due to the electric field is responsible for the non-Ohmic behavior. We assume for simplicity that only carriers in the conduction band contribute to the ultrasonic attenuation because of their large mobility.

As the degenerate temperature for $n=1.5\times 10^{13}$ cm⁻³ is about 2°K, and n in the conduction band in the low-electric-field limit may be supposed less than 10^{12} cm⁻³ (as will be shown later), we assume that our sample is in the nondegenerate state at 4.2°K. Since the mobility of electrons in the low-electric-field limit is about 10^5 cm²/V sec (as also shown later), the carriers are in the quantum limit for magnetic fields much higher than 400 G. On the other hand, in the high electric field the carriers are heated up to about 20°K owing to electric fields,¹² so that the carriers are not in the quantum limit unless the magnetic field is much higher than 2 kG.

If we assume ionized impurity scattering to be predominant, ω_s and ω_D in Eq. (4) in strong magnetic fields ($\omega_c\tau > 1$) are given by the following relations for the quantum limit¹³ and the classical case¹⁰:

$$\omega_s = (\rho_0\epsilon)^{-1}(\omega_c\tau)^{-2}B, \quad \omega_D = (qv_s^2/\mu_0kT)[(\omega_c\tau)^2/B], \quad (5)$$

$$B = \frac{8}{\pi} \frac{\ln[(4kT + \epsilon_s)/\hbar\omega_c] + \ln(\epsilon_s/\hbar\omega_c)}{\ln[1 + (12kT/\epsilon_s)] - [1 + (\epsilon_s/12kT)]^{-1}} \ln(kT/\epsilon_c), \quad (6a)$$

(quantum limit)

$$= 3.40, \quad (\text{classical limit}) \quad (6b)$$

where ρ_0 and μ_0 are the resistivity and the mobility in the absence of magnetic field, respectively, ω_c is the cyclotron frequency, τ is the relaxation time, $\epsilon_s = \hbar^2q_s^2/2m^*$, $q_s = (4\pi q^2n/\epsilon kT)^{1/2}$ is the Debye screening wave number, m^* ($=0.013m$) is the effective mass, and $\epsilon_c = [\hbar^2\omega_c/\tau(kT)^{1/2}]^{2/3}$ is the cutoff energy due to collision broadening.

Let us compare the experiment for 43 MHz in Fig. 2 with the results calculated based on Eqs. (5) and (6). In the small-amplitude limit, the piezoelectric field $|E_s|$ is less than 0.2 V/cm as obtained from Tables I and II and Eq. (3), so that the experimental curve can be analyzed by using the Ohmic resistivity $\rho=370$ Ω cm and Eq. (6a). In Fig. 4 are shown the experimental curve and three theoretical curves $\mu=1.0\times 10^6$ for (a), $\mu=1.35\times 10^5$ (b), and $\mu=2.0\times 10^5$ cm²/V sec (c). The theoretical curves are insensitive to the resistivity

¹¹ Y. Katayama and S. Tanaka, Phys. Rev. **153**, 873 (1967).

¹² H. Miyazawa, J. Phys. Soc. Japan **26**, 700 (1969).

¹⁰ Y. Abe and N. Mikoshiba, J. Appl. Phys. (Japan) **7**, 881 (1968); C. Hervouet, Phys. Status Solidi **21**, 117 (1967); M. C. Steel, RCA Rev. **28**, 58 (1967).

¹³ E. N. Adams and T. D. Holstein, J. Phys. Chem. Solids **10**, 254 (1959). See also L. M. Roth and P. N. Argyres, in *Semiconductors and Semimetals*, edited R. K. Willardson and A. C. Beer (Academic Press Inc., New York, 1966), Vol. 1, p. 159.

around $\rho=370 \Omega \text{ cm}$. From the best-fit curve (b) we estimate $\mu=1.35 \times 10^5 \text{ cm}^2/\text{V sec}$ and $n=1.3 \times 10^{11} \text{ cm}^{-3}$ in the low electric field. The fitting, however, is not satisfactory. The discrepancy between experiment and theory seems to come from the neglect of contribution of carriers in the impurity band.

For the analysis of experiment in the large-amplitude limit, we shall take tentatively an effective resistivity $\rho_{\text{eff}}=9 \Omega \text{ cm}$ at $H=0$. In Fig. 5 are shown the experimental curve and three calculated curves using Eq. (6b), $T=20^\circ\text{K}$, $\mu=1.3 \times 10^5$ for (A), $\mu=1.55 \times 10^5$ (B), and $\mu=1.7 \times 10^5 \text{ cm}^2/\text{V sec}$ (C). From the best fit curve (B) we have the approximate values of $\mu=1.55 \times 10^5 \text{ cm}^2/\text{V sec}$ and $n=8 \times 10^{12} \text{ cm}^{-3}$.¹⁴ It should be noted that the calculated curves are insensitive to the carrier temperature T between 10 and 20°K but vary a little with the resistivity. If we change the value of ρ from 6 to $10 \Omega \text{ cm}$, the mobility giving the best-fit curve changes from 1.7×10^5 to $1.4 \times 10^5 \text{ cm}^2/\text{V sec}$.

For the typical amplitude-dependent attenuation shown in Fig. 1, we cannot analyze the data in a simple

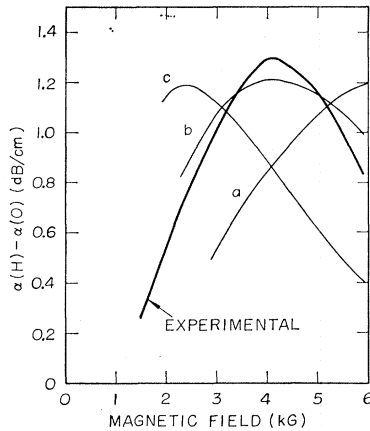


FIG. 4. Comparison of the experimental and calculated curves for the small-amplitude limit. The calculated curves are given for the cases that $\omega=2.7 \times 10^8$, $\rho=3.7 \times 10^2 \Omega \text{ cm}$, and (a) $\mu=1.0 \times 10^5$; (b) $\mu=1.35 \times 10^5$; (c) $\mu=2.0 \times 10^5 \text{ cm}^2/\text{V sec}$.

¹⁴ The Hall coefficient R under the magnetic field of 140 G at 4.2°K was $9.7 \times 10^6 \text{ cm}^3/\text{C}$ and $1.6 \times 10^6 \text{ cm}^3/\text{C}$ for the dc electric field of 0.1 V/cm (Ohmic region) and 0.8 V/cm (non-Ohmic region), respectively. Though one cannot estimate the carrier concentration from R straightforwardly in the two-band model, the decrease in R reflects the increase in the effective carrier concentration. This fact is qualitatively consistent with the present analysis.

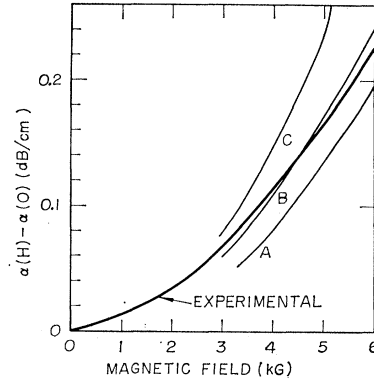


FIG. 5. Comparison of the experimental and calculated curves for the large amplitude case. The calculated curves are given for the cases that $\omega=2.7 \times 10^8$, $\rho=9 \Omega \text{ cm}$, and (A) $\mu=1.3 \times 10^5$; (B) $\mu=1.55 \times 10^5$; (C) $\mu=1.7 \times 10^5 \text{ cm}^2/\text{V sec}$.

way as discussed before. However, we can understand general features of Fig. 1 in the following way. We obtain $\omega_s=2.3 \times 10^8 \text{ sec}^{-1}$ for $\rho=2.7 \times 10^3 \Omega \text{ cm}$ at $E_s < 0.4 \text{ V/cm}$ (small-amplitude limit) and $\omega_s=6 \times 10^{10} \text{ sec}^{-1}$ for $\rho=10 \Omega \text{ cm}$ at $E_s > 1 \text{ V/cm}$ (large-amplitude limit). For the ultrasonic wave of 160 MHz ($\omega \cong 10^9 \text{ sec}^{-1}$), the calculations based on Eq. (4) show that we have the nearly incomplete screening case in the small-amplitude limit, while the large-amplitude limit belongs to the nearly complete screening case. This explains the opposite dependence on the magnetic field of attenuations in the small and large amplitude.

In conclusion, the amplitude-dependent attenuation found in *n*-InSb is ascribed to the non-Ohmic behavior of electrical conduction at low temperatures. Comparing the acoustic experiments with the theory, we found that the change in mobility at low and high electric fields is not large enough to explain the non-Ohmic-resistivity-versus-field measurements. The non-Ohmic effect in our sample may be due to the repopulation of carriers between the impurity and conduction bands.

ACKNOWLEDGMENTS

The authors wish to thank Dr. M. Kikuchi and H. Hayakawa for supplying the sample of InSb. The authors are indebted to the members of Solid State Physics Group for their support given in the course of this work. They are also indebted to Dr. H. Miyazawa for receiving an advance copy of his work.